

Effects of Simulated Microgravity on the Development of the Swimbladder and Buoyancy Control in Larval Zebrafish (*Danio rerio*)



BENJAMIN W. LINDSEY¹, TRISTAN C. DUMBARTON²,
STEPHEN J. MOORMAN³, FRANK M. SMITH¹, AND ROGER P. CROLL^{2*}

¹Department of Anatomy and Neurobiology, Dalhousie University, Halifax, Nova Scotia, Canada

²Department of Physiology and Biophysics, Dalhousie University, Halifax, Nova Scotia, Canada

³Department of Neuroscience and Cell Biology, Robert Wood Johnson Medical School, Piscataway, New Jersey

ABSTRACT

The gas-filled swimbladder of teleost fishes provides hydrodynamic lift which counteracts the high density of other body tissues, and thereby allows the fish to achieve neutral buoyancy with minimal energy expenditure. In this study, we examined whether the absence of a constant direction gravitational vector affects the ontogeny of the swimbladder and buoyancy control in zebrafish (*Danio rerio*). We exposed fertilized eggs to simulated microgravity (SMG) in a closed rotating wall vessel with control eggs placed in a similar but nonrotating container. All eggs hatched in both groups. At 96 hr of postfertilization (hpf), all larvae were removed from the experimental and control vessels. At this point, 62% of the control larvae, but only 14% of SMG-exposed larvae, were observed to have inflated their swimbladder. In addition, the mean volume of the inflated swimbladders was significantly greater in the control larvae compared with larvae raised in SMG. After transfer to open stationary observation tanks, larvae with uninflated swimbladders in both groups swam to the surface to complete inflation, but this process was significantly delayed in larvae exposed to SMG. Initial differences in swimbladder inflation and volume between groups disappeared by 144 hpf. Furthermore, there were no apparent changes in patterns of development and maturation of swimbladder musculature, vasculature, or innervation resulting from SMG exposure at later stages of ontogeny. These data indicate that, despite a transient delay in swimbladder inflation in zebrafish larvae exposed to SMG, subsequent swimbladder development in these animals proceeded similarly to that in normal larvae. *J. Exp. Zool.* 315:302–313, 2011. © 2011 Wiley-Liss, Inc.

How to cite this article: Lindsey BW, Dumbarton TC, Moorman SJ, Smith FM, Croll RP. 2011. Effects of simulated microgravity on the development of the swimbladder and buoyancy control in larval zebrafish (*Danio rerio*). *J. Exp. Zool.* 315:302–313.

J. Exp. Zool.
315:302–313, 2011

Grant Sponsor: Canadian Space Agency; Grant numbers: 9F007-0460116; 9F007-071237; Grant Sponsor: Natural Sciences and Engineering Council Discovery grants to RPC and FMS and a Canadian Institutes of Health studentship award to TCD.

The present address of Benjamin W. Lindsey is Department of Cell and Systems Biology, University of Toronto, Toronto, ON, Canada M5S 3G5.

Frank M. Smith and Roger P. Croll contributed equally to this manuscript.

*Correspondence to: Roger P. Croll, Department of Physiology and Biophysics, Dalhousie University 5850 College Street Halifax, NS, Canada B3H 1X5. E-mail: Roger.Croll@Dal.ca

Gravitational force provides a fixed frame of reference for three-dimensional orientation of organisms at the surface of the Earth, but this frame of reference is largely absent in microgravity. Studies conducted on vertebrates during space travel (Snetkova et al., '95; Sebastian and Horn, '98; Anken et al., 2000; Wiederhold et al., 2000; Hilbig et al., 2002; Ijiri, 2003; Walton

Received 13 August 2010; Revised 29 December 2010; Accepted 7 February 2011

Published online in Wiley Online Library (wileyonlinelibrary.com). DOI: 10.1002/jez.677

et al., 2005; Horn, 2006a,b), parabolic flights (Wassersug and Izumi-Kurotani, '93), or ground-based simulated microgravity (SMG) (Moorman et al., '99, 2002; Nishikawa et al., 2005; Shimada et al., 2005) have shown that the normal physiology of many organs in the body depends on gravitational force with a constant direction and magnitude. This phenomenon is readily apparent in astronauts who, after space flight, exhibited short and long-term dysfunctions of the vestibular, cardiovascular, endocrine, and musculoskeletal systems (Edgerton et al., '95; Vernikos, '96; Strollo, '99).

Despite a growing body of knowledge on the influence of microgravity on organ physiology, the impact of microgravity on developmental processes remains poorly understood (National Research Council, '98; Dournon, 2003; Izumi-Kurotani and Kiyomoto, 2003). The development of the gravity-sensing organs of the vestibular apparatus stands as a notable exception, having received much attention across vertebrates. In particular, recent work on otolith development in teleost fishes has clarified our perception of the relationship between gravitational input and otolith development (Anken et al., 2000; Wiederhold et al., 2000; Moorman et al., 2002). However, fish must also be able to perceive their depth and actively compensate for changes in buoyancy, as their position changes in the water column. These organisms thus have additional demands placed on their ability to orient to gravity when compared with terrestrial vertebrates. Nearly half of extant teleost fishes possess a gas-filled swimbladder that provides lift to offset the high density of bone and muscle tissues. Fish can continuously adjust the volume of gas in this organ to establish neutral buoyancy at a specific depth in the water column, thereby reducing the energy that would otherwise be expended in swimming to maintain that depth (Denton, '61; Steen, '70; Gee and Holst, '92; Alexander, '93; Webber et al., 2000). In addition to its critical function in determining the orientation of fish in the water column, the swimbladder also seems to play an important, but poorly understood, role in the successive development of other organs. If inflation of the swimbladder during early larval development is prevented, larvae subsequently display developmental abnormalities (Chatain and Corrao, '92; Goolish and Okutake, '99) and have reduced survival rates (Friedmann and Shutty, '99; Czesny et al., 2005; Trotter et al., 2005) in a variety of teleost species.

In order to better understand the development of the swimbladder and its contribution to three-dimensional orientation, we have begun to exploit zebrafish as a model organism. Recently, we described the stereotypical process of swim-up behavior leading to swimbladder inflation in early zebrafish larvae (Lindsey et al., 2010) and the anatomical details of subsequent development of this organ (Robertson et al., 2007). The larvae hatch at 48–72 hr postfertilization (hpf) and initial inflation of the swimbladder normally occurs within the first 96 hpf. This is accomplished when larvae break the surface to gulp air (Lindsey et al., 2010), which is then passed into the

swimbladder via the pneumatic duct (Steen, '70; Rieger and Summerfelt, '98; Lindsey et al., 2010). The first innervation and vascularization of the swimbladder appear at approximately 144 hpf (Robertson et al., 2007). Following evagination of the second (anterior) chamber from the cranial aspect of the original (now posterior) chamber, distinct bands of smooth muscle coalesce on the lateral aspects of the posterior chamber and the ventral aspect of the anterior chamber at 3–4 weeks postfertilization. Muscle development is accompanied by maturation of local vasculature and innervation, and these events likely mark the beginning of functional control of swimbladder volume by autonomic reflexes (Nilsson, 2009; Smith and Croll, 2010) acting on the maturing effectors.

The proper progression, through the initial inflation of the swimbladder and subsequent development, might be hypothesized to depend upon a consistent gravitational force that would be reflected in changes in whole animal buoyancy. Indeed, some reports suggest that abnormal swimbladder inflation occurs in adult and larval fish aboard space flights (Anken et al., 2000; Ijiri, 2003), where microgravity would eliminate normal sensory feedback for buoyancy control mechanisms. However, no studies to date have investigated changes either in behaviors associated with swimbladder inflation or in the morphology of the swimbladder, following exposure to altered gravitational forces.

The aim of this study was to determine whether initial swimbladder inflation, subsequent anatomical development of this organ, and swimming behavior were disrupted, following exposure of zebrafish eggs and larvae to SMG through the use of a rotating wall vessel (RWV), designed by the U.S. National Aeronautics and Space Administration to explore the effects of SMG on cell cultures, but recently adapted for studies on zebrafish eggs (Moorman et al., '99). Our findings suggest that, although SMG can have transient effects on early stages of the development of buoyancy control, the swimbladder system of zebrafish is highly robust and seems to rapidly compensate for any disruptions in development that may be caused by early exposure to SMG. Moreover, these experiments further demonstrate that the effects of orbital microgravity can be at least partially replicated in SMG, thus opening the door for more detailed ground-based studies on developmental mechanisms underlying anatomy, physiology, and behavior in conditions of altered gravity.

MATERIALS AND METHODS

Animals

Adult wild type zebrafish (*Danio rerio*) were obtained from local suppliers (AquaCreation, Halifax, NS, Canada) and then bred and maintained in our laboratory facility using established procedures (Westerfield, '95). All experiments were approved by the Dalhousie University Animal Care Committee and followed the animal use guidelines of the *Canadian Council on Animal Care*. Animals were kept on a 14 hr light (from 08:00 h): 10 hr dark

cycle in aquaria supplied with 28°C recirculating and dechlorinated tap water. Eggs were collected daily within the first 2 hr of the light cycle. One portion of each batch of eggs was immediately placed into the RWV for exposure to SMG and an equivalent portion of eggs was placed in a stationary vessel as controls.

Rotating Wall Vessel and Control Vessel

The RWV (Synthecon, Houston, TX), which was used to simulate microgravity, consisted of a transparent and hollow Lexan cylinder (10 cm O.D.) forming a water-filled chamber of approximately 250 mL surrounding a solid inner core of Teflon (5 cm I.D.; Fig. 1). The cylinder was closed at both ends by Teflon caps. One of the caps was fitted with ports for access to the water in the vessel, through which fertilized eggs were transferred at the start of experiments, and the other cap was attached to a shaft coupled to a variable speed motor that rotated the cylinder around a horizontal axis at a rate between 8.5 and 26.5 rpm (revolution per minute⁻¹). The cylindrical control vessel consisted of an isovolumetric and transparent replicate of the RWV, but it was not rotated; instead, it was placed upright on the base of the RWV, so that zebrafish eggs in the control group were subjected to the same vibration and light stimuli as those in the experimental group.

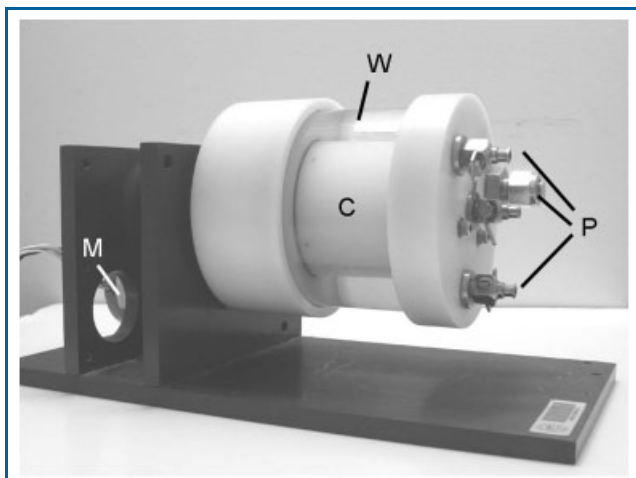


Figure 1. Rotating wall vessel (RWV) used to simulate microgravity. The rotor consisted of a clear outer Lexan cylinder permitting observations of zebrafish eggs in the water (W) in the chamber surrounding the core (C). The rotor was turned at a constant rate of 18.5 rpm by a stepping motor (M) to maintain eggs in a circular orbit in relation to the core. Ports (P) allowed access to the water in the chamber for insertion of fertilized eggs or removal of air bubbles after briefly stopping rotation as the experiment progressed. Larvae in the control group were placed in a vessel with similar dimensions to the RWV (not shown).

Exposure of Zebrafish Eggs to Simulated Microgravity

The RWV was filled with dechlorinated tap water that was in equilibrium with atmospheric oxygen and that contained 0.0005% (w/v) methylene blue to prevent fungal growth (Westerfield, '95). A maximum of 50 fertilized eggs was placed into the vessel for each experimental trial, air bubbles were removed, and the chamber was sealed and mounted on the RWV base. The speed of rotation was adjusted to ensure that the eggs, observed through the chamber wall, were maintained in a nearly circular orbit around the core of the vessel. This orbit indicated that the magnitudes of the gravitational and centrifugal force vectors were balanced, providing a resultant net directional force vector near zero (for review and underlying mathematical principles, see Moorman et al., 2002). In our experiments, the rate of rotation giving this effect was 18.5 rpm. Controls, as described above, were run simultaneously with each experimental trial.

Zebrafish eggs and larvae were exposed to experimental or control conditions at 28°C for 96 hr hpf. The RWV was stopped briefly (maximum 3 min) 1–2 times per day to remove air bubbles, which might give upward directional cues, disrupt the circular orbit of the eggs, or possibly facilitate swimbladder inflation once larvae hatched. Ammonia, nitrite, and nitrate levels along with pH of the water were monitored using commercial kits (Aquarium Pharm Inc., Lancaster, PA), and dissolved oxygen content (Model 5850 Dissolved Oxygen Meter; Yellow Springs Instruments Co., Inc, Yellow Springs, OH) and water temperature were measured. Measurements were made on samples of fresh tap water used to fill the vessels and immediately after removal of larvae from the closed vessels at 96 hpf.

The summary of all experiments, including treatment conditions and sample sizes, is given in Table 1.

Total Body Length and the Inflation and Volume of the Swimbladder

After 96 hr exposure to the experimental ($n = 70$) or control ($n = 42$) conditions, larvae intended for measurements of swimbladder development were immediately sacrificed by placing 0.02% w/v MS-222 (ethyl 3-aminobenzoate methanesulfonate salt; Sigma Chemical Co., Mississauga, ON, Canada) directly into the RWV or control vessel. This prevented possible inflation of the swimbladder during subsequent handling of the larvae. Once animals had ceased all movement, total body length (tip of lower jaw to the end of the caudal fin) was measured and the presence or absence of an inflated swimbladder was recorded. A digital photograph of the lateral view of the swimbladder was taken through the transparent body wall of those larvae in which this organ was inflated (Fig. 2a, inset). From this image, the lengths of the short and long axes of the swimbladder were measured and the volume estimated using the equation for a rotary prolate ellipsoid, $V = 4/3 \pi ab^2$, where $a = 0.5$ long axis and $b = 0.5$ short axis (Robertson et al., 2008).

Additional groups of experimental ($n = 18$) and control ($n = 17$) larvae were transferred at 96 hpf from the vessels without anesthetic to stationary aquaria (9 cm high \times 9 cm

Table 1. Experimental conditions and sample sizes for all experiments.

Experiment Developmental characteristics examined	Group	Age (stage) at time of observation/sacrifice	Sample size
Total body length, swimbladder inflation, swimbladder volume	Experimental (SMG)	96 hpf	70
	Control (1-G)	96 hpf	42
Swim-up behavior	Experimental (SMG)	144 hpf	18
	Control (1-G)	144 hpf	17
Swimming depth	Experimental (SMG)	96–144 hpf	60
	Control (1-G)	96–144 hpf	64
Neuromuscular and vascular anatomy of the swimbladder	Experimental (SMG)	8 dpf (ESC)	24
	Control (1-G)	8 dpf (ESC)	24
	Experimental (SMG)	25 dpf (LDC)	19
	Control (1-G)	25 dpf (LDC)	12
Neuromuscular and vascular anatomy of the swimbladder	Experimental (SMG)	8 dpf (ESC)	60
	Control (1-G)	8 dpf (ESC)	38
	Experimental (SMG)	25 dpf (LDC)	8
	Control (1-G)	25 dpf (LDC)	8

All larvae were raised in closed vessels for 96 hpf during exposure to either simulated microgravity (SMG) or normal 1-G. Larvae were examined between 96 hpf and up to 8 or 25 days postfertilization (dpf), when they were at the Early Single Chamber (ESC) or Late Double Chamber (LDC) stage, respectively.

long × 9 cm wide), where they were maintained until 144 hpf. Upon reaching this age, animals were sacrificed and their swimbladder volumes and total body lengths determined for comparison with larvae at 96 hpf.

Swim-Up Behavior

The swimming behaviors of larvae exposed to experimental or control conditions were video-recorded in the same 9 cm deep aquaria, as described above. Recordings commenced shortly after larvae were transferred from the RWV or control vessel at 10:00 h (2 hr into the light cycle) and continued during daylight hours for two consecutive days until all fish were free-swimming in the water column. Approximately 15 larvae were video-recorded at a time to yield $n = 60$ experimental and $n = 64$ control larvae recorded for swim-up behavior. All video recording was performed using a CCD video camera (Honeywell Model HCM574E, Syosset, NY) aimed at the front of each tank and connected to a computerized digital recording system (Astra 8 Video Surveillance System, Pace Setter Technologies Inc., Dartmouth, NS, Canada). The depth of individuals from the surface of the water was scored once every hour to the nearest centimeter and the average depth of all larvae in each group calculated and plotted for each hour of the recording period.

Long-Term Effects on Swimming Depth

Additional larvae were transferred from the RWV or control vessel at 96 hpf and reared under stationary ambient conditions in the 9 cm deep aquaria for either an additional 4 days until reaching body lengths of 3.5–4.0 mm, at which point they were at the early

single chamber (ESC) stage, or an additional 3 weeks until reaching body lengths of 9.5–10 mm, at which point they were at the late double chamber (LDC) stage (Robertson et al., 2007). The ESC larvae (experimental, $n = 24$; control, $n = 24$) were then video-recorded, as described above, over a single 1 hr session in the 9 cm deep tank and swimming depth was subsequently scored to the nearest centimeter at 6 min intervals. The LDC larvae (experimental, $n = 19$; control, $n = 12$) were transferred to an observation tank, 36 cm high × 25 cm long × 25 cm wide, and left for an additional 30 min acclimation period before video-recording and subsequent scoring of swimming depth.

Neuromuscular and Vascular Anatomy of the Swimbladder

The anatomical development of the swimbladder of larvae exposed to SMG during the first 96 hpf was evaluated histologically at the ESC (experimental, $n = 60$; control, $n = 38$) and LDC stages (experimental, $n = 8$; control, $n = 8$). After removal from the RWV or control vessel, fish were raised and killed, as described above. The swimbladders were removed by dissection and fixed in 4% paraformaldehyde in phosphate-buffered saline (PBS; 50 mM Na_2HPO_4 , 140 mM NaCl; pH 7.2) at room temperature for 2 hr. Tissues were subsequently rinsed three times with PBS for 45 min before further histochemical processing.

The presence and organization of myocytes within the swimbladder were visualized by incubating tissues overnight with phalloidin (1:100 dilution) conjugated to tetramethylrhodamine-isothiocyanate (TRITC; Sigma Chemical Co., Mississauga, ON, Canada) to label F-actin (Small et al., '99). Tissues were then

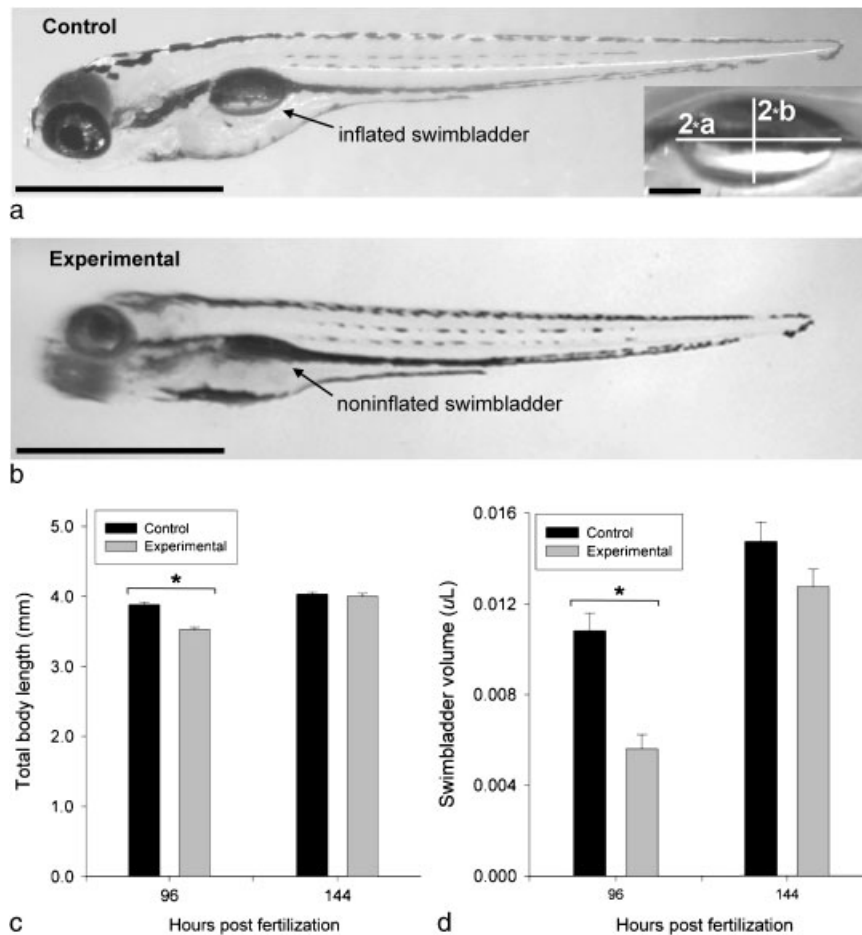


Figure 2. Effects of SMG on swimbladder morphology, total body length, and swimbladder volume during development. **a, b:** Representative photomicrographs of left lateral views of larvae with inflated swimbladders from control (**a**) and larvae with uninflated swimbladders from experimental (**b**) groups at 96 hpf. Inset shows magnified view of single-chambered swimbladder with the long (2*a) and short (2*b) axes marked for volumetric analysis, as modeled by a rotary prolate ellipsoid (see text). In **b**, the arrow marks the position of the uninflated swimbladder in larvae exposed to SMG. In all images of swimbladder in this and subsequent figures, cranial is to the left and dorsal is upward. **c:** Plots of total body length of larvae from control (black bars; $n = 42$) and experimental (gray bars; $n = 70$) groups measured at 96 and 144 hpf (control: $n = 17$; experimental: $n = 18$). **d:** Plots of swimbladder volumes estimated from animals that had inflated swimbladders at 96 hpf (control: $n = 26$; experimental: $n = 10$) and 144 hpf (control: $n = 17$; experimental: $n = 18$) with bar shading as in **c**. Asterisk (*) indicates a significant difference (independent samples t -test, $P < 0.001$) in mean values between groups at the same time point. In panels **a** and **b**, scale bars represent 1.0 mm; in inset, 100 μm .

rinsed in PBS and mounted on microscope slides in a solution of three parts glycerol to one part 0.1 M Tris buffer (pH 8.0) containing 2% n-propyl gallate (Giloh and Sedat, '82). Blood vessels were labeled with a polyclonal antibody raised in goat against Tie-2 (1:200 dilution; R & D Systems, Minneapolis, MN), a receptor tyrosine kinase expressed primarily in endothelial and hematopoietic progenitor cells (Lyons et al., '98). To visualize the swimbladder innervation, the monoclonal antibody zn-12 (1:100 dilution; Developmental Studies Hybridoma Bank, Iowa City, IA) was used as a general zebrafish neuronal marker (Metcalf et al.,

'90). Both primary antibodies were diluted in PBS with 0.5% Triton X-100 and tissues were incubated for 7–10 days at 4°C. Negative controls were obtained by omitting primary antibody from the incubation solutions. Further details of the specificity of Tie-2 and zn-12 labeling in the zebrafish swimbladder are outlined in Robertson et al. (2008). Following incubation with primary antibodies, tissues were rinsed three times with PBS for 45 min and placed in PBS containing 0.5% Triton X-100 and fluorescein-tagged anti-mouse (for zn-12) or anti-goat (for anti-Tie-2) secondary antibodies (1:50 dilution). Tissues were

incubated in the dark for 4 days at 4°C, and then rinsed with PBS and mounted on microscope slides in a buffered glycerol solution, as described above.

Digital images were taken using a Zeiss LSM 510 confocal laser-scanning microscope. Confocal z-stacks of 20–40 images captured at 0.5–2.0 µm intervals were projected to create single images using proprietary Zeiss software. All images were adjusted for consistency of brightness and contrast and assembled into plates using Photoshop 7.0 (Adobe Systems, Inc., San Jose, CA).

Statistical Analysis

Values are expressed as mean ± 1 standard error. The significance level for all statistical evaluations of difference was set at $P \leq 0.05$. Levene's and Komolgorov-Smirnov tests were performed to examine the parametric assumptions of equal variances and normality, respectively. Paired comparisons were done using independent or paired sample *t*-tests, as noted. Statistical procedures were performed with SPSS 14.0 (SPSS Inc., Chicago, IL).

RESULTS

Total Body Lengths of Larvae and the Inflation and Volumes of Their Swimbladders

At 96 hpf, control larvae were about 10% longer than larvae raised in SMG (Fig. 2a–c; independent samples *t*-test, $P < 0.001$). The majority (62%) of larvae in the control group had inflated their swimbladders by 96 hpf, whereas only 14% of the larvae raised in SMG had inflated swimbladders by this time. Of those larvae with an inflated swimbladder, the mean volume of the organ was significantly greater in control larvae compared with those exposed to SMG (Fig. 2d; independent samples *t*-test, $P < 0.001$). By 144 hpf (after all larvae had been raised in stationary tanks for 48 hr), all fish in both groups had inflated swimbladders, and there was no longer any significant difference between mean volume of swimbladders in control and experimental larvae (independent samples *t*-test, $P = 0.088$) nor between the mean total body length of the larvae in the two groups.

Swim-Up Behavior and Swimming Depths at ESC and LDC Stages

There were no mortalities in either the experimental or control group of larvae that were used to observe swim-up behavior. All control larvae with inflated swimbladders at 96 hpf were free-swimming and generally located just beneath the surface of the water immediately after being transferred to the 9 cm deep observation tank. The remaining control larvae, in which the swimbladders were not inflated at 96 hpf, were attached at varying depths to the walls of the observation tank. Over the next several hours, the larvae moved progressively closer to the surface and by 100 hpf had inflated their swimbladders and were free-swimming near the surface of the water. These trends are represented in Figure 3 by the gradual decrease in mean depth of

control larvae (filled circles) from 97 to 100 hpf and maintenance of a consistent mean depth of larvae thereafter.

Those larvae that were raised in SMG and that had inflated swimbladders (14%) were also free-swimming just under the surface, after transfer to the observation tank at 96 hpf. However, the majority of larvae had not inflated their swimbladders and were positioned on the bottom of the observation tank after transfer from the RWV. The mean depth for all larvae in the experimental group at 97 hpf (Fig. 3, first open circle) was thus significantly deeper than the initial depth of control larvae (independent samples *t*-test, $P < 0.0001$). Within the first 3 hr of observation, larvae in the experimental group that were on the tank bottom began moving toward the surface and displaying stereotypical swim-up behavior (Lindsey et al., 2010). By 100 hpf, when all control larvae had reached the surface and inflated their swimbladders, the mean depth of larvae in the experimental group was still significantly deeper than that of control animals (independent samples *t*-test, $P < 0.0001$) and remained so until 108 hpf. Over the following day (starting at 119 hpf), the remaining larvae slowly ascended to the surface and, by 126 hpf, had attained a relatively shallow mean depth that remained unchanged over the rest of the observation period. By 133 hpf, all larvae in the experimental group had filled their swimbladders and were free-swimming, but at a mean depth that was significantly deeper than that of control larvae during this period (Fig. 3; $P = 0.007$).

By 4 days after transfer from the RWV or control vessel (i.e., at 192 hpf), larvae from both groups had reached the ESC stage and occupied statistically similar mean swimming depths (independent samples *t*-test, $P = 0.592$) (Fig. 4). Similarly, animals

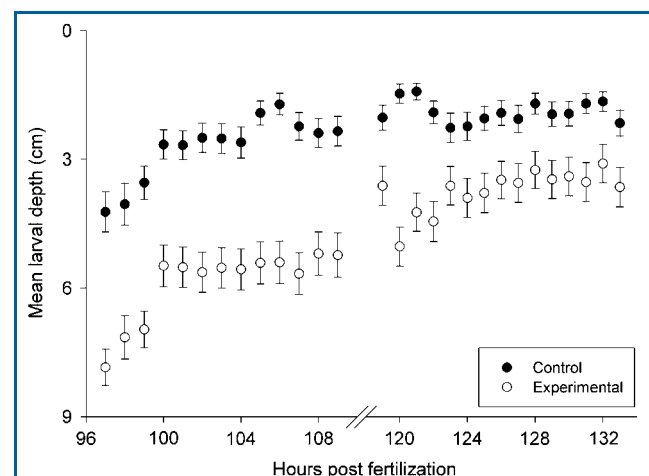


Figure 3. Mean depth of larvae during swim-up behavior over the first 36 hr after transfer from the RWV (open circles: $n = 60$) or control vessel (closed circles: $n = 64$) to the 9 cm deep observation tank. The break in the horizontal axis indicates the dark portion of the photoperiod when no observations were made.

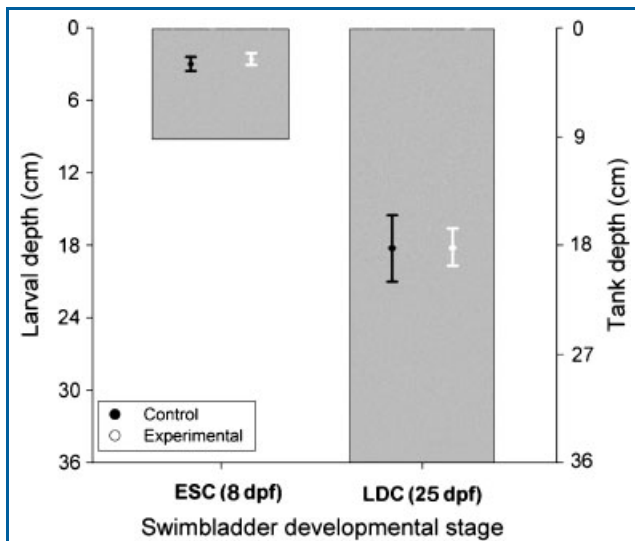


Figure 4. Changes in mean swimming depth (left vertical scale) of larval zebrafish in control (black circles: $n = 24$) and experimental (white circles: $n = 24$) groups at ESC (8 dpf) and LDC (21 dpf; experimental: $n = 19$; control: $n = 12$) stages of swimbladder development. Values are means calculated from a 1 hr video recording session at the two developmental stages. The gray shaded bars indicate total depth of the observation tanks (right vertical scale) used for recordings at each stage. There were no significant differences between these groups at either stage (independent samples t -tests, $P > 0.05$).

exposed to SMG, before being raised to the late double chamber (LDC) stage, also displayed no statistically significant difference in mean depth from control fish when viewed in a 36 cm deep observation tank (Fig. 4; independent samples t -test, $P = 0.967$).

Swimbladder Anatomy

The anatomy of the swimbladder was similar in specimens in the control ($n = 38$) and experimental ($N = 60$) groups at the ESC stage, and consistent with previous reports (Robertson et al., 2007). Specifically, phalloidin revealed diffuse labeling with no discernable myocytes or muscle bands in swimbladders of specimens of either group (Fig. 5a and b, and insets). Tie-2-like immunoreactivity demonstrated similar patterns of vasculature in the ESC stage of larvae of both groups, with anastomosing capillary loops extending laterally in the walls of the anterior end of the swimbladder (Fig. 5c and d). In both groups, zn-12 immunoreactivity revealed two large nerves extending caudally within the lateral walls of the swimbladder from its cranial aspect, converging at the caudal most protuberance (Fig. 5e and f). At higher magnification, numerous varicosities could be seen on the axonal processes branching from the lateral nerves (Fig. 5g and h). The size of the lateral nerves, the branching patterns of the fiber tracts, and the presence of varicosities did

not seem to differ between swimbladders sampled from the two groups.

By 3 weeks after exposure to SMG, the swimbladders in both the control ($N = 8$) and experimental ($N = 8$) groups clearly demonstrated a constricted communicating duct and an anterior chamber which was larger than the posterior chamber. These features, as shown in Figure 6a and b, indicate that all fish had entered the LDC stage, as would be expected by that age (Robertson et al., 2007). There also did not seem to be any anatomical differences between these groups in patterns of musculature in the posterior chamber. Lateral muscle bands in both groups were composed of a thick layer of circumferentially oriented smooth muscle fibers overlain by a thinner layer of longitudinal fibers (Fig. 6c and d, details shown in insets). Anti-Tie-2 did not label the more developed vasculature at this stage, but phalloidin staining revealed smooth muscle associated with blood vessels in the posterior chambers of both groups. Vessels entered the swimbladder wall close to the junction between the pneumatic duct and posterior chamber, and coursed along lateral muscle bands in parallel arrangements of venules and arterioles (Fig. 6e and f). The innervation of the posterior chamber of the swimbladder consisted of large bilateral axonal tracts with smaller tracts dispersed in the wall of the anterior chamber in both groups (Fig. 6g and h, inset). All swimbladder innervation seemed to originate from two large nerves, one coursing along the pneumatic duct and the other along the swimbladder artery. Clusters of putative neuronal cell bodies were observed in the walls of both chambers in close association with some axons (i.e., at arrow in inserts, Fig. 6g and h).

Water Quality in Closed Vessels From 0 to 96 hpf

Water chemistry variables in the RWV and control vessels after 96 h larval occupancy are shown in Table 2, in comparison with levels of the same variables at the start of each experiment. pH in both vessels decreased slightly from that of tap water. Ammonium, nitrate, and nitrite were present in undetectable amounts in tap water, but all these compounds were detected in the RWV after 96 hr. Only ammonium and nitrite were detected in the control vessel after 96 hr. Mean levels of ammonium and nitrate were not significantly different between the two vessels (independent samples t -test, $P > 0.05$). The mean concentration of dissolved oxygen was near the level of saturation at the start of each experiment, but decreased after 96 hr by 22 and 45% in the control vessel and RWV, respectively. These differences from initial value were significant in both cases (paired sample t -test, $P = 0.006$), but the mean levels of oxygen in each vessel at the end of the experiment were not significantly different from each other (independent samples t -test, $P = 0.118$).

DISCUSSION

This study demonstrates that zebrafish embryos and larvae exposed to SMG for 96 hpf subsequently exhibited a delay in

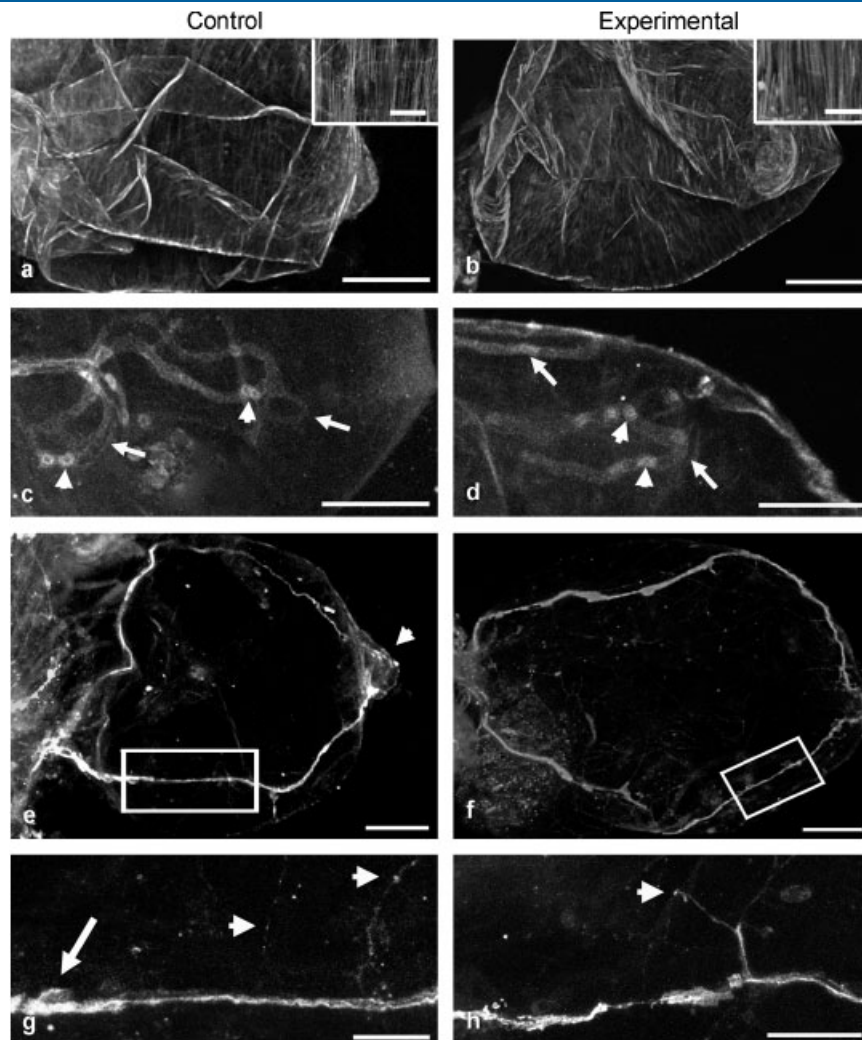


Figure 5. Anatomy of swimbladders from larvae at the ESC stage of swimbladder development. Panels a, c, e, g show images taken from swimbladders of control group ($n = 38$); panels b, d, f, h show images from swimbladders of experimental group ($n = 60$). b, c (insets show higher magnification views): Phalloidin labeling showed that no swimbladder muscular development was present in either group. c, d: Tie-2-like immunoreactivity showed blood vessels extending along the walls and ending in anastomotic loops (arrows) in swimbladders from both groups. Erythrocytes are visible within some vessels (arrowheads). e, f: In both groups, zn-12 immunoreactivity showed paired lateral nerves coursing to the cranial end of the swimbladder, then along the walls bilaterally before converging caudally at the apex (arrowhead). g, h: Details of regions shown within boxes in panels e and f. Numerous fine ramifications arose from lateral nerves in specimens from both groups; a putative cell body (arrow) was associated with a lateral nerve in the sample from the control group, although these cells were also observed in tissue from the experimental group (data not shown). In tissue from both groups, intensely stained structures resembling varicosities (arrowheads) occurred along many fibers. Scale bars represent: a, b, 50 μm (inset, 20 μm); c–f, 50 μm ; g, h, 10 μm .

swim-up behavior compared with control animals. This delay was accompanied by other short-term disruptions in development, including decreased swimbladder volume and body length. However, behavior, swimbladder morphology, and body size were similar between the experimental and control groups by 144 hpf. Furthermore, no long-term effects of SMG on the anatomy of swimbladder musculature, vasculature, or

innervation were detected in animals examined 4 days or 3 weeks following termination of the SMG exposure.

Swim-Up Behavior, Swimbladder Inflation, and Volume

Access to the air–water interface seems to be essential for initial swimbladder inflation in the larvae of most teleosts (Steen, '70; Alexander, '93). Specifically, Goolish and Okutake ('99) have

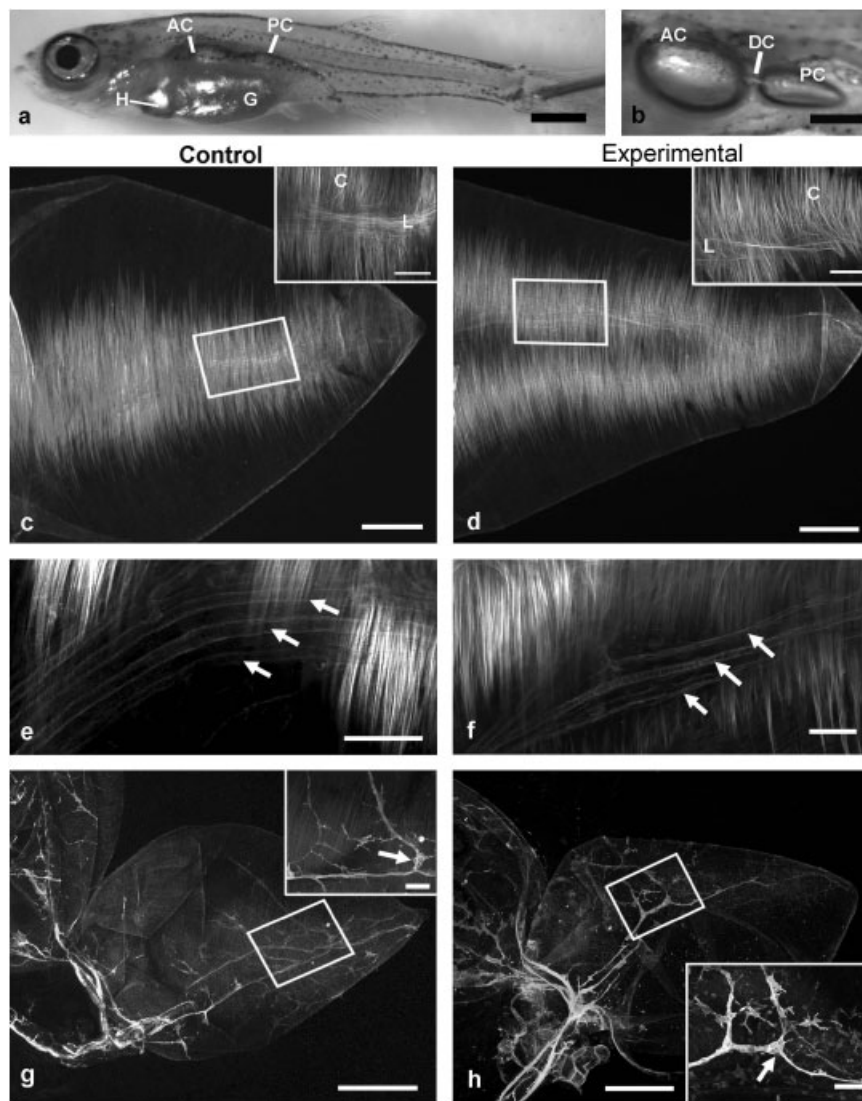


Figure 6. Anatomy of larval swimbladders from control ($n = 8$) and experimental ($n = 8$) groups at the LDC stage of development. **a:** Representative larva from control group (total body length 9.5 mm) showing anterior (AC) and posterior (PC) chambers of swimbladder in relation to the gut (G; partly obscuring swimbladder) and heart (H). **b:** Higher magnification image of swimbladder in situ in opened coelomic cavity; AC and PC connected by a narrowed ductus comunicans (DC). Panels **c, e, g** show images of tissues from control group; **d, f, h** show images of tissue from experimental group. **c, d:** Phalloidin labeled smooth muscle fibers of lateral muscle bands in the wall of the PC in both groups. Boxes in main panels show locations of insets, which depict circular (C) and longitudinal (L) muscle fibers. **e, f:** Smooth muscle was associated with blood vessels of the rete (arrows), as demonstrated by phalloidin labeling in the wall of craniolateral portion of the PC in tissue from both groups. **g, h:** Zn-12 immunoreactivity showed robust neuronal staining within the walls of both swimbladder chambers and in nerves coursing to the swimbladder along the pneumatic duct (arrowhead). In each panel, insets show details of regions indicated by boxes; putative neuronal cell bodies were observed in swimbladders from both control and experimental groups (arrows). Scale bars represent: **a,** 1 mm; **b,** 0.5 mm; **c, d,** 100 μm (insets, 50 μm); **e, f,** 50 μm ; **g, h,** 200 μm (insets, 50 μm).

shown that zebrafish larvae prevented from accessing the surface generally do not inflate the swimbladder (see below), and no evidence has been found for structures that could support the active transfer of gas from the blood into the swimbladder in

either adult (Finney et al., 2006) or larval (Robertson et al., 2008) zebrafish. Thus, swimbladder inflation in this species seems to be entirely dependent on access to air. And yet, despite efforts to keep the RWV and control vessel free of air bubbles, the majority

Table 2. Water chemistry variables sampled from dechlorinated tap water.

Water sample	Temperature (°C)	pH	Ammonium (ppm)	Nitrite (ppm)	Nitrate (ppm)	Dissolved O ₂ (mg O ₂ /L)
Dechlorinated tap water	24.9 ± 0.29	7.2	0	0	0	7.65 ± 0.12
Control vessel	28.2 ± 0.87	6.9 ± 0.1	0.13 ± 0.13	0	2.5 ± 2.5	*5.94 ± 0.55
Rotating wall vessel	27.2 ± 0.17	6.5 ± 0.12	0.33 ± 0.12	0.06 ± 0.06	4.5 ± 1.2	*4.19 ± 0.65

Quality of water used to initially fill the rotating wall vessel and control vessel and after zebrafish larvae had occupied these chambers for 96 hpf. Values are expressed as mean ± standard error. Asterisk indicates significant differences between tap water mean value and mean values recorded in water samples after 96 hpf.

of control larvae and even some experimental larvae had inflated their swimbladders by 96 hpf. These findings were consistent with those of Goolish and Okutake ('99), who previously suggested that zebrafish can fill their swimbladders by gulping air from microbubbles that form on the walls of closed vessels lacking an air-water interface. However, despite the fact that some animals from both groups inflated their swimbladders by the end of the trial period, our study demonstrated a significant difference between the experimental and control groups in the number of larvae with inflated swimbladders. A possible explanation for this difference between the groups could be that the bubbles forming on the walls of the control vessel were stationary relative to the larvae and could, therefore, be more easily accessed than those in the RWV, which were continually moving in relationship to the larvae.

Previous studies in other aquatic species have reported changes in swimbladder inflation and buoyancy after return to 1-G from space orbit, similar to those we report here. For instance, neither the swimbladders of newly hatched swordtail fish larvae (Anken et al., 2000) nor the lungs of newly hatched tadpoles of the African clawed frog (Souza et al., '95) were initially inflated upon return from space flights. Moreover, both the larval fish and tadpoles were situated on the bottom of the observation tanks immediately after transfer from the flight vessels after landing. Within a few days, however, these animals had inflated their swimbladders or lungs, and subsequently displayed normal swimming behaviors. It has been suggested that difficulties in organ inflation under these conditions may be owing to a reduced capability of the larvae to orient toward and pierce the air-water interface in microgravity (Snetkova et al., '95; Souza et al., '95; Wassersug and Yamashita, 2000). The changes in swimbladder inflation and larval position in the water column, which we observed after transferring zebrafish larvae from the RWV to the stationary observation tank, were thus consistent with observations of fish and frogs upon return to 1-G from space, and suggest that the larvae encountered similar problems in SMG. A likely cause for the lack of swimbladder inflation in SMG (as well as in actual microgravity encountered on space flights) is that without a reliable gravitational vector, the saccule and utricle within the vestibular apparatus can no longer function as reliable monitors of body orientation in

relation to the air-water interface. This is supported by earlier reports demonstrating that rearing fertilized zebrafish eggs in the same RWV, as used here, caused developmental abnormalities of the larval vestibular system (Moorman et al., '99, 2002). The larvae, therefore, have difficulty moving toward the surface and perhaps also fail to respond appropriately to gulp air when they reach the air-water interface. In fact, studies of vestibular dysfunction caused by the *monolith* mutation in zebrafish have shown that the bilateral loss of utricular otoliths disrupts the ability of larvae to sense gravity and severely impairs balance and coordination, leading to a reduction in the number of animals capable of inflating their swimbladders (Riley and Moorman, 2000).

Once larvae were moved from the RWV to the stationary observation tanks, those animals that had not yet inflated their swimbladders initiated this process, but full inflation then took several additional hours to complete. Much of this delay likely occurred simply because the larvae needed to first complete swim-up behavior to attain the surface of the water, a process which itself may occupy several hours (see Fig. 3; Lindsey et al., 2010). However, it is also possible that some of the delay occurred because of residual effects of SMG exposure on otolith development or general vestibular dysfunction (Rahmann and Anken, 2000; Riley and Moorman, 2000; Wiederhold et al., 2003). An additional factor which may have influenced the onset of swim-up behavior in the experimental animals was a general retardation in the rate of body growth, as typified here by shorter mean body length after SMG exposure. It has been previously established that stages of swimbladder development are tightly linked with whole-body length in zebrafish and that swimbladder inflation does not usually occur before animals have grown to a minimum total body length of 3.5 mm (Robertson et al., 2008), although swim-up behavior may begin earlier (Lindsey et al., 2010). In this study, the mean total body length of larvae treated in the RWV was significantly shorter than that of control larvae at 96 hpf (Fig. 2).

A final factor that may have affected swimbladder inflation in our study was the water quality. Levels of nitrogenous metabolites did not increase significantly, whereas levels of oxygen fell significantly in the vessels which were closed for 96 hr (Table 2). The number of replicates was low in our study,

however, and the power of the statistical analyses may simply have been inadequate to detect such changes. It is, therefore, not clear what the biological effects of changes in water quality were. Water quality seems to be seldom, if ever, monitored in space flights (Shimura et al., 2004). Our study is the first to attempt to examine water quality in ground-based studies of SMG exposure on teleosts and suggests that such measures deserve more attention in the future.

Long-Term Effects of SMG

Our findings indicated that the initial deficits in swimbladder inflation and volume arising from exposure to SMG lasted no longer than 48 hr after removal from the RWV. There was no significant difference in swimbladder volume at 144 hpf nor in the swimming depth of larvae at EDC and LDC stages, between the treatment groups (Fig. 4). We also found no evidence that SMG exposure induced changes in the structure of the swimbladder wall. There were no gross morphological differences in the swimbladders of the two groups at the ESC and LDC stages nor were there any obvious differences in patterns of innervation, musculature, or vasculature at these stages of development (Figs. 5 and 6); the appearance of these anatomical patterns were similar to those reported by Robertson et al. (2007) for the zebrafish swimbladder at the same stages. The swimbladder system of the zebrafish has thus been shown to be highly robust in response to external disruptions of normal gravitational stimulation at 0–96 hpf, a finding that is consistent with previous work on other species. For instance, after returning to Earth from a 16-day exposure to microgravity in space, adult and larval swordtail fish exhibited short-term disruptions in swimming behavior (presumably owing to a deflated swimbladder), but this behavior returned to normal within 1 day of landing (Anken et al., 2000).

Concluding Remarks

These experiments were designed to assess the effects of SMG exposure during early development on buoyancy control. Ground-based studies of the effects of SMG are essential for the establishment of guidelines for experimental design that may be realized during future space flights, especially given the recent development of research facilities aboard the International Space Station (Brinckmann, 2003). However, developmental studies involving SMG still remain challenging, as the methods available for ground-based research are limited by either short exposure periods or the physical constraints of a closed system, such as the RWV used in this study. Our findings provide a foundation for the development of further methodologies to investigate the effects of longer term SMG on development in vertebrate species. The results of such studies will ultimately facilitate the design of protocols to investigate the biology of organisms over a full life cycle in microgravity conditions.

LITERATURE CITED

- Alexander RM. 1993. Buoyancy. In: Evans DH, editor. The physiology of fishes. Boca Raton: CRC Press. p 75–97.
- Anken RH, Hilbig R, Ibsch M, Rahmann H. 2000. Readaptation of fish to 1g after long-term microgravity: behavioural results from the STS 89 mission. *Adv Space Res* 25:2019–2023.
- Brinckmann E. 2003. New facilities and instruments for developmental biology research in space. *Adv Space Biol Med* 9:253–280.
- Chatain B, Corrao D. 1992. A sorting method for eliminating fish larvae without functional swimbladders. *Aquaculture* 107:81–88.
- Czesny SJ, Graeb BDS, Dettmers JM. 2005. Ecological consequences of swim bladder noninflation for larval yellow perch. *Trans Am Fish Soc* 134:1011–1020.
- Denton EJ. 1961. The buoyancy of fish and cephalopods. *Prog Biophys Biophys Chem* 11:178–234.
- Dournon C. 2003. Developmental biology of urodele amphibians in microgravity conditions. *Adv Space Biol Med* 9:101–131.
- Edgerton VR, Zhou MY, Ohira Y, Klitgaard H, Jiang B, Bell G, Harris B, Saltin B, Gollnick PD, Roy RR, Daly MK, Greenisen M. 1995. Human fiber size and enzymatic properties after 5 and 11 days of spaceflight. *J Appl Physiol* 78:1733–1739.
- Finney JL, Robertson GN, McGee CAS, Smith FM, Croll RP. 2006. Structure and autonomic innervation of the swimbladder in the zebrafish (*Danio rerio*). *J Comp Neurol* 495:587–606.
- Friedmann BR, Shutty KM. 1999. Effect of timing of oil film removal and first feeding on swim bladder inflation success among intensively cultured striped bass larvae. *N Am J Aquacult* 61:43–46.
- Gee JH, Holst HM. 1992. Buoyancy regulation by sticklebacks *Culaea inconstans* and *Pungitius pungitius* in response to different salinities and water densities. *Can J Zool* 70:1590–1594.
- Giloh H, Sedat JW. 1982. Fluorescence microscopy: reduced photobleaching of rhodamine and fluorescein protein conjugates by n-propyl gallate. *Science* 217:1252–1255.
- Goolish EM, Okutake K. 1999. Lack of gas bladder inflation by the larvae of zebrafish in the absence of an air–water interface. *J Fish Biol* 55:1054–1063.
- Hilbig R, Anken RH, Sonntag G, Hohne S, Henneberg J, Kretschmer N, Rahmann H. 2002. Effects of altered gravity on the swimming behaviour of fish. *Adv Space Res* 30:835–841.
- Horn ER. 2006a. Microgravity-induced modifications of the vestibulo-ocular reflex in *Xenopus laevis* tadpoles are related to development and the occurrence of tail lordosis. *J Exp Biol* 209:2847–2858.
- Horn ER. 2006b. *Xenopus laevis*—a success story of biological research in space. *Adv Space Res* 38:1059–1070.
- Ijiri K. 2003. Life-cycle experiments of medaka fish aboard the international space station. *Adv Space Biol Med* 9:201–216.
- Izumi-Kurotani A, Kiyomoto M. 2003. Morphogenesis and gravity in a whole amphibian embryo and in isolated blastomeres of sea urchins. *Adv Space Biol Med* 9:83–99.
- Lindsey BW, Smith FM, Croll RP. 2010. From inflation to flotation: contribution of the swimbladder to whole-body density and

- swimming depth during development of the zebrafish (*Danio rerio*). Zebrafish 7:85–96.
- Lyons MS, Bell B, Stainier D, Peters KG. 1998. Isolation of the zebrafish homologues for the tie1 and tie-2 endothelium-specific receptor tyrosine kinases. Dev Dyn 212:133–140.
- Metcalfe WK, Myers PZ, Trevarrow B, Bass MB, Kimmel CB. 1990. Primary neurons that express the L2/HNK-1 carbohydrate during early development in the zebrafish. Development 110:491–504.
- Moorman SJ, Burrell C, Cordova R, Slater J. 1999. Stimulus dependence of the development of the zebrafish (*Danio rerio*) vestibular system. J Neurobiol 38:247–258.
- Moorman SJ, Cordova R, Davies SA. 2002. A critical period for functional vestibular development in zebrafish. Dev Dyn 223:285–291.
- National Research Council. 1998. A strategy for research in space biology and medicine in the new century. Part II: physiology, gravity, and space. Washington, DC: National Academy Press.
- Nilsson S. 2009. Nervous control of fish swimbladders. Acta Histochem 111:176–184.
- Nishikawa M, Ohgushi H, Tamai N, Osuga K, Uemura M, Yoshikawa H, Myoui A. 2005. The effect of simulated microgravity by three-dimensional clinostat on bone tissue engineering. Cell Transplant 14:829–835.
- Rahmann H, Anken RH. 2000. Gravitational neurobiology of fish. Adv Space Res 25:1985–1995.
- Rieger PW, Summerfelt RC. 1998. Microvideography of gas bladder inflation in larval walleye. J Fish Biol 53:93–99.
- Riley BB, Moorman SJ. 2000. Development of utricular otoliths, but not saccular otoliths, is necessary for vestibular function and survival in zebrafish. J Neurobiol 43:329–337.
- Robertson GN, McGee CA, Dumbarton TC, Croll RP, Smith FM. 2007. Development of the swimbladder and its innervation in the zebrafish, *Danio rerio*. J Morphol 268:967–985.
- Robertson GN, Lindsey BW, Dumbarton TC, Croll RP, Smith FM. 2008. The contribution of the swimbladder to buoyancy in the adult zebrafish (*Danio rerio*): a morphometric analysis. J Morphol 269:666–673.
- Sebastian C, Horn E. 1998. The minimum duration of microgravity experience during space flight which affects the development of the roll induced vestibulo-ocular reflex in an amphibian (*Xenopus laevis*). Neurosci Lett 253:171–174.
- Shimada N, Sokunbi G, Moorman SJ. 2005. Changes in gravitational force affect gene expression in developing organ systems at different developmental times. BMC Dev Biol 5:10.
- Shimura R, Ma YX, Ijiri K, Nagaoka S, Uchiyama M. 2004. Nitrate toxicity on visceral organs of medaka fish, *Oryzias latipes*: aiming to raise fish from egg to egg in space. Biol Sci Space 18:7–12.
- Small J, Rottner K, Hahne P, Anderson KI. 1999. Visualising the actin cytoskeleton. Microsc Res Tech 47:3–17.
- Smith FM, Croll RP. 2010. Autonomic innervation of the swimbladder. Auton Neurosci DOI: 10.1016/j.autneu.2010.08.002.
- Snetkova E, Chelnaya N, Serova L, Saveliev S, Cherdanzova E, Pronych S, Wassersug R. 1995. Effects of space flight on *Xenopus laevis* larval development. J Exp Zool (Mol Dev Evol) 273:21–32.
- Souza KA, Black SD, Wassersug RJ. 1995. Amphibian development in the virtual absence of gravity. Proc Natl Acad Sci USA 92:1975–1978.
- Steen JB. 1970. The swim bladder as a hydrostatic organ. In: Hoar WS, Randall DJ, editors. Fish physiology. New York: Academic Press. p 413–443.
- Strollo F. 1999. Hormonal changes in humans during spaceflight. Adv Space Biol Med 7:99–129.
- Trotter AJ, Pankhurst PM, Battaglione SC. 2005. A finite interval of initial swimbladder inflation in *Latris lineata* revealed by sequential removal of water surface films. J Fish Biol 67:730–741.
- Vernikos J. 1996. Human physiology in space. Bioessays 18:1029–1037.
- Walton KD, Benavides L, Singh N, Hatoum N. 2005. Long-term effects of microgravity on the swimming behaviour of young rats. J Physiol 565:609–626.
- Wassersug R, Izumi-Kurotani A. 1993. The behavioral reactions of a snake and a turtle to abrupt decreases in gravity. Zoolog Sci 10:505–509.
- Wassersug RJ, Yamashita M. 2000. The mechanics of air-breathing in anuran larvae: implications to the development of amphibians in microgravity. Adv Space Res 25:2007–2013.
- Webber DM, Aitken JP, O'Dor RK. 2000. Costs of locomotion and vertic dynamics of cephalopods and fish. Physiol Biochem Zool 73:651–662.
- Westerfield M. 1995. The zebrafish book: a guide for the laboratory use of zebrafish (*Brachydanio rerio*). Eugene, OR: University of Oregon Press.
- Wiederhold ML, Harrison JL, Parker KA. 2000. A critical period for gravitational affects on the formation of otoliths in swordtail fish. Grav Space Biol Bull 14:66.
- Wiederhold ML, Harrison JL, Gao W. 2003. A critical period for gravitational effects on otolith formation. J Vestib Res 13:205–214.